Physics design of collimators to reduce lost particle background at the CEPC

Teng Yue(岳腾) Qing-Lei Xiu(修青磊) Yi-Wei Wang(王毅伟) Zhe Duan(段哲) Qing Qin(秦庆)

Key Laboratory of Particle Acceleration Physics and Technology, Institute of High Energy Physics, CAS, Beijing 100049, China

Abstract: At the CEPC (Circular Electron Positron Collider), which is proposed by the Chinese high energy physics community, the dominant background comes from radiative Bhabha scattering and the beamstrahlung effect according to preliminary research. Therefore, it is necessary to incorporate a collimator system to intercept particles that may be lost near the interaction region (IR). In this paper, we introduce some limitations in choosing the position and width of the collimators. A certain parameter range is determined which is confined by the β function and the width of the collimators. A suitable choice of the half width is made by exploring this parameter range. A simulation of the particle loss rate in the IR and the hit density in the vertex detector with and without the collimators shows that the set of parameters of the collimators we designed is appropriate and effective.

Keywords: CEPC, lost particle background, collimator

PACS: 29.20db, 29.27.-a **DOI:** 10.1088/1674-1137/40/11/117001

1 Introduction

After the discovery of the Higgs boson at the LHC [1,2], proposals have been put forward to build a circular Higgs factory such as FCC-ee [3] or CEPC [4] to measure the properties of this new particle precisely. The CEPC (Circular Electron Positron Collider) is a ring-based Higgs factory proposed by the Chinese high energy physics community. It will be operated at a center-of-mass energy of about 240 GeV, and the peak luminosity will be greater than 10^{34} cm^{-2}s^{-1}, according to the Preliminary Conceptual Design Report (Pre-CDR) [4]. The extremely high commissioning energy means the particles that are lost near the IR also carry much energy. Hence, particle showers resulting from the interaction between the lost particles and the vacuum chamber or detector component will become more significant. These primary and secondary particles will lead to substantial background in the detectors and must be evaluated carefully. Based on preliminary research [5], the dominant background sources in CEPC are driven by radiative Bhabha scattering and beamstrahlung. The design of the collimators aims at these two effects at this stage.

To achieve the shielding effect, the collimator should be placed close enough to the beam orbit. On the other hand, a distance that is too small may induce the transverse mode coupling instability. Especially for the CEPC, the width of the collimators in the vertical plane should be large enough for vertical injection. Taking these limiting conditions into consideration, along with the results of simulations of the accelerator and detectors, we propose a set of optimized parameters of the collimators. In addition, we perform the simulation of the particle loss rate in the IR and the hit density in the vertex detector with and without the collimators. The simulation results demonstrate that the collimators are effective.

2 The geometric design of the collimators

In general, the geometric design of a collimator can be illustrated by the sketch in Fig. 1. The left-hand plot of Fig. 1 shows the side view of a collimator. The half width of the chamber tapers from r (the half width of beam pipe) to d (the half width of the collimator, here we take the vertical for example). The taper angle α is small in general to keep this chamber as smooth as possible. Otherwise, the transverse mode coupling instability may become serious. The length of the collimator is L and the middle part of it is L_d. The right-hand plot illustrates the view in the plane transverse to the beam direction, representing two kinds of collimator aperture, round and rectangular, respectively. The design of the CEPC collimators is be modelled with the rectangular aperture. d_x and d_y are the half width of the collimator in the horizontal and vertical directions respectively.

Received 28 March 2016, Revised 28 April 2016

©2016 Chinese Physical Society and the Institute of High Energy Physics of the Chinese Academy of Sciences and the Institute of Modern Physics of the Chinese Academy of Sciences and IOP Publishing Ltd

3 Constraints on the width and position of the collimators

Since the dominant background sources originate from radiative Bhabha scattering and the beamstrahlung effect, the collimators are incorporated to intercept the background due to these two effects. The position of the collimators should satisfy the following constraints on the half width and the β function where they are located. Some parameters of CEPC are listed in Table 1.

3.1 Upper limit on the half width

The half width of a collimator should be small enough to shield the particles that may reach the IR. In other words, the ratio between the half width and the beam size at the place where the collimator is located should be smaller than that in the IR

$$d_{\rm c}\Big/\sqrt{\varepsilon\beta_{\rm c}} \leqslant r_{\rm IR,min}\Big/\sqrt{\varepsilon\beta_{\rm IR,max}}. \tag{1}$$

In Eq. (1), ε is the transverse emittance, $d_{\rm c}$ and $\beta_{\rm c}$ are the half width and β function in the collimator, $r_{\rm IR,min}$ is the minimum radius of the pipe in the IR and $\beta_{\rm IR,max}$ is the maximum β function in the IR. The horizontal and vertical plane should be considered separately. According to Eq. (1), the upper limit of the half width of the collimator can be expressed as

$$d_{\rm c} \leqslant \frac{r_{\rm IR,min}}{\sqrt{\beta_{\rm IR,max}}}\sqrt{\beta_{\rm c}}. \tag{2}$$

Based on the IR design at this stage with $r_{\rm IR,min}$ of 1.7 cm, the maximum horizontal beta function in the IR is about 64.374m and that in the vertical plane is about 1191.778 m. Subsequently, we can get the upper limit at the collimator from the Eq. (2) in the horizontal and vertical plane respectively.

3.2 Limit from the transverse mode coupling instability (TMCI)

A collimator that is too close to the beam orbit gives rise to increasingly dramatic effects from the transverse mode coupling instability, also referred to as the fast head-tail instability or strong head-tail instability. This provides an upper limit to the bunch current [6]

$$I_{\rm thresh} = \frac{C_1 f_{\rm s} E/e}{\sum\limits_i \beta_i k_i(\sigma_z, d)}, \tag{3}$$

where C_1 is a constant with a value of about 8, $f_{\rm s}$ is the synchrotron frequency, E is the beam energy and k is the kick factor of the collimator. For CEPC, the reference value of the collimator taper angle is 0.11 rad. This value results in the intermediate regime for a rectangular collimator. So the kick factor can be analytically written [7, 8] as

$$k = 0.215AZ_0c\sqrt{\frac{\alpha}{\sigma_z d^3}} \tag{4}$$

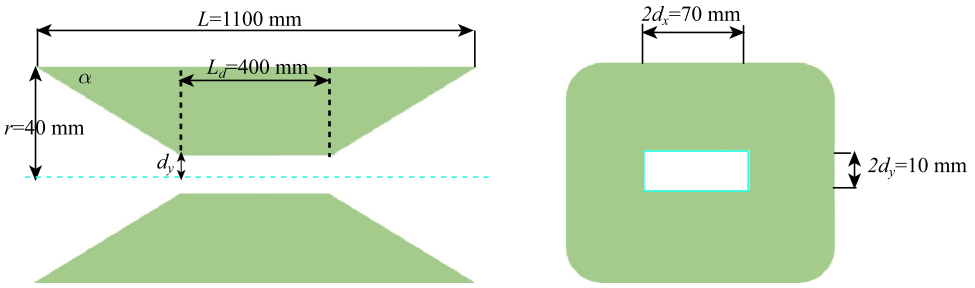

Fig. 1. The side and transverse view of a collimator.

Table 1. Some parameters of CEPC.

parameters	units	value
beam energy [E]	GeV	12
luminosity [L]	cm^{-2}·s^{-1}	1.69E34
circumference [C]	km	54.88
energy acceptance [η]		2%
emittance-horizontal [$\varepsilon_{\rm x}$]	m·rad	6.12E-09
emittance-vertical [$\varepsilon_{\rm y}$]	m·rad	1.84E-11
betax at IP [$\beta_{\rm x}$]	m	0.8
betay at IP [$\beta_{\rm y}$]	m	0.003
lifetime due to Radiative bhabha scattering [$\tau_{\rm RBB}$]	min	52
lifetime due to beamstrahlung [$\tau_{\rm BS}$]	min	47

In Eq. (4), A is a constant (about 1), Z_0 is the impedance of free space (about 377 Ω) and α represents the taper angle shown in Fig. 1, which has a value of roughly 0.11 for CEPC. Substituting Eq. (4) into Eq. (3), one can get a lower limit on the half width of the collimator

$$d_{\rm c} \geqslant \left(\frac{0.215AIZ_0c}{C_1 f_{\rm s} E/e}\right)^{\frac{2}{3}} \left(\frac{\alpha}{\sigma_z}\right)^{\frac{1}{3}} \beta_{\rm c}^{\frac{2}{3}}. \tag{5}$$

The threshold bunch current should be larger than 332 μA, while the total current is about 16.6 mA and there are 50 bunches along the whole ring. Note that Eq. (5) is derived with the assumption that only one collimator is mounted. For the multi-collimator condition, the kick factor of different collimators in Eq. (3) should be added together.

3.3 Vertical injection requirement

Different from the horizontal plane, the half width of the collimator in the vertical plane should be large enough to allow vertical injection [9], so that the influence of injection on the pretzel orbit can be avoided. The injected beam and the circulating beam are shown as follows.

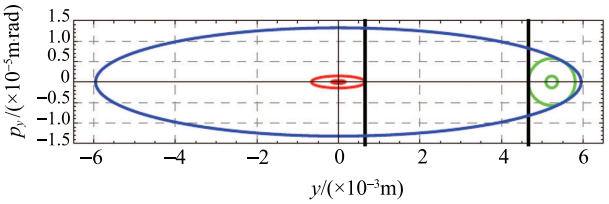

Fig. 2. (color online) Sketch of the injected beam and the circulating beam in phase space.

In Fig. 2, the central red ellipse shows the circulating beam and the green ellipse on the right represents the injected beam. The outer blue ellipse is the acceptance ellipse we define. The beam size is considered as 4 times the standard deviation of the Gaussian distribution in the vertical plane in the definition. The distance between these two beams is preliminarily set to 4 mm. The acceptance in the vertical plane is hence determined to be about 7.88×10^{-8} m.rad and the half width of the collimator in the vertical plane should satisfy the following equation:

$$d_{{\rm c},y} \geqslant \sqrt{a_y \beta_{{\rm c},y}}. \tag{6}$$

3.4 Allowed parameter range for the collimators

The beta function of CEPC is shown in the plot below (Fig. 3), where the blue curve is β_x and the green one is β_y. The x-axis represents the distance to the interaction point. This figure demonstrates half of the IR, with several FODO cells and the conjunction region between them. The β_x varies from 0 m to 243 m and β_y from 0 m to 1220 m.

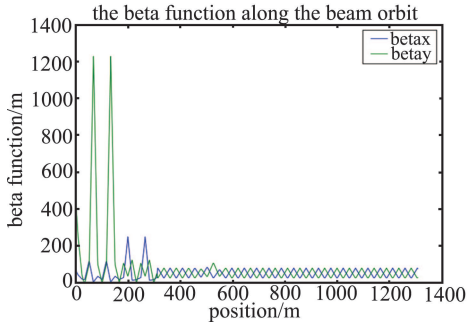

Fig. 3. (color online) The beta function along the beam orbit.

a) Design of the horizontal collimators

For the design of the collimators in the horizontal plane, the constraints mentioned in Sections 1 and 2 must be taken into consideration. According to Eq. (2) and Eq. (5), one can get

$$\begin{cases} d_{{\rm c},x} \leqslant \dfrac{r_{{\rm IR},\min}}{\sqrt{\beta_{{\rm IR},x,\max}}}\sqrt{\beta_{{\rm c},x}} \\ d_{{\rm c},x} \geqslant \left(\dfrac{0.215AIZ_0c}{C_1 f_{\rm s} E/e}\right)^{\frac{2}{3}} \left(\dfrac{\alpha}{\sigma_z}\right)^{\frac{1}{3}} \beta_{{\rm c},x}^{\frac{2}{3}} \end{cases}. \tag{7}$$

The parameter space allowed is as shown in Fig. 4.

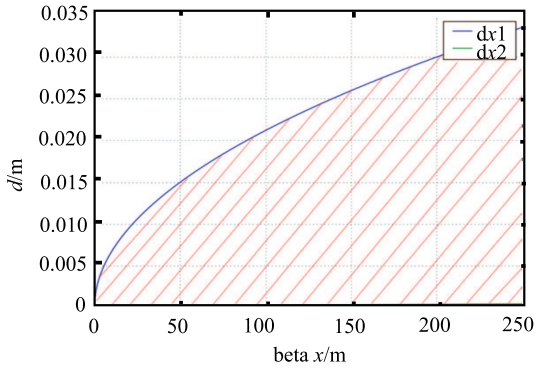

Fig. 4. (color online) The parameters allowed for the collimators in the horizontal plane.

Figure 4 shows the parameters allowed for the collimators in the horizontal plane. The upper blue line gives the aperture constraint mentioned in Section 1 and the lower green line shows the TMCI condition. The hatched region between them represents the allowed region in the parameter space. Additionally, the place we choose should be a long straight drift which can accommodate collimators. According to the lattice design of the CEPC, we decide to install the horizontal collimators at the DRHS22FFS.4, which is 266.412 m upstream of the IR, and DRHS12FFS.4, which is 200.412 meters upstream of the IR. The β_x at both these points is about

238.9 m. The distance between them is about 66 m and the phase advance is π. Based on Fig. 4, the allowed half width in these places is in the range of 0.6 to 34.1 mm.

b) Design of the vertical collimators

Unlike the design of the collimators in the horizontal plane, we should also take the injection constraint into consideration in designing the vertical collimators. According to Eq. (2), Eq. (5) and Eq. (6), one can write

$$\begin{cases} d_{c,y} \leqslant \dfrac{r_{\mathrm{IR,min}}}{\sqrt{\beta_{\mathrm{IR},y,\mathrm{max}}}}\sqrt{\beta_{c,y}} \\ d_{c,y} \geqslant \left(\dfrac{0.215AIZ_0c}{C_1 f_s E/e}\right)^{\frac{2}{3}} \left(\dfrac{\alpha}{\sigma_z}\right)^{\frac{1}{3}} \beta_{c,y}^{\frac{2}{3}} \\ d_{c,y} \geqslant \sqrt{a\beta_{c,y}} \end{cases} . \quad (8)$$

The allowed region in the parameter space is shown in Fig. 5. The colour scheme used in Fig. 5 is similar to that in Fig. 4, with an additional black line between the two curves mentioned above representing the constraint given by the injection condition. The hatched region is the candidate parameter space. According to the lattice design of CEPC, we decide to install the vertical collimators at DRHFFS.7, which is 283.212 meters upstream of the IR, and DRHFFS.8, which is 217.212 meters upstream of the IR. The β_y at both these points is about 124.05 meters. The distance between them is about 66 meters with a phase advance of π. Based on Fig. 5, the allowed half width is 3.3 mm $< d <$ 5.4 mm.

Furthermore, the half width should better be kept away from the line confined by the TMCI condition, because the actual number of collimators is more than one, which is our assumption when determining the constraints.

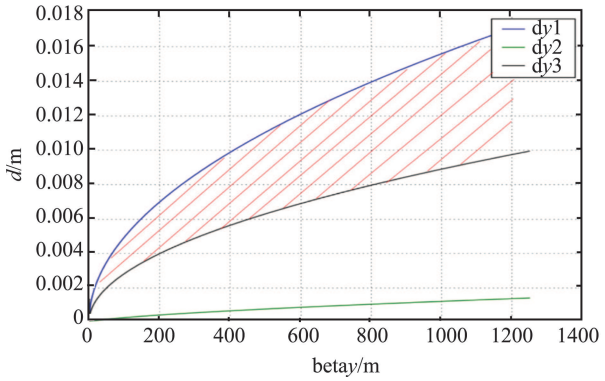

Fig. 5. (color online) The parameters allowed for the collimators in the vertical plane.

4 Scan of collimator half widths

Table 2 summarizes the parameters of the collimators determined from the analysis in previous section.

A simulation of the loss rate in the IR with different half widths was performed, using BBBREM [10] and a tracking algorithm developed based on SAD [11]. As an example, the simulation results of the radiative Bhabha scattering are shown in Fig. 6. Only the electron beam is simulated in this paper. The simulation result of the positron beam is thought symmetric to that of the electron beam, as the lattice is symmetric for these two beams.

Table 2. Summary of collimator parameters.

name	position	distance to IP/m	beta function/m	range of half width allowed/mm
APTX1	DRHS12FFS.4	−200.412	β_x = 238.91	0.6–34.1
APTX2	DRHS22FFS.4	−266.412	β_x = 238.91	0.6–34.1
APTY1	DRHFFS.7	−283.212	β_y= 124.05	3.3–5.4
APTY2	DRHFFS.8	−217.212	β_y = 124.05	3.3–5.4

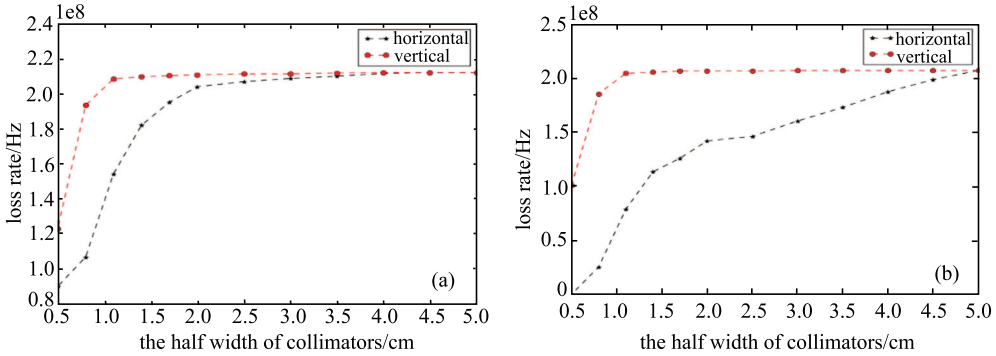

Fig. 6. (color online) Loss rate in the IR from radiative Bhabha scattering with different half widths of the collimators at the two IPs: (a) scattering originating from IP1 and (b) from the IP3.

Figure 6 shows the loss rate originating from radiative Bhabha scattering simulated in the IR with different half widths of the collimators. Figure 6 (a) and Fig. 6 (b) show the simulation result with radiative Bhabha scattering originating from IP1 and IP3, respectively. In both plots, the black stars represent the results in the horizontal plane and the red circles those in the vertical plane. Figure 6 implies that there is almost no effect on the loss rate when the width is larger than 1.1 cm in the vertical plane and the lower loss rate needs a smaller half width. In the horizontal plane, however, especially at IP3, the loss rate decreases significantly with a narrower gap. Overall, we set the half width of the collimators to 8 mm and 5 mm in the horizontal and vertical plane respectively. With this gap design and four collimators mounted (two for the horizontal plane and two for the vertical plane), the TMCI condition can still be satisfied.

According to Table 1, the lifetime due to beamstrahlung is as serious as that driven by radiative Bhabha scattering. So, we should also simulate beamstrahlung. The simulation method for the background arising from beamstrahlung is similar to that for simulating the radiative Bhabha scattering background, except that the Monte Carlo generator is developed based on the formula of beamstrahlung-driven lifetime [12, 13].

Figure 7, similar to Fig. 6, shows the loss rate simulated in the IR originating from beamstrahlung with different half widths of the collimators, with Fig.7 (a) and Fig. 7 (b) showing the simulation results with the background source at IP1 and IP3 respectively. As a whole, the loss rate due to beamstrahlung without the collimators is about a quarter of that from radiative Bhabha scattering. The loss rate decreases significantly with a narrower gap.

The simulation of the loss rate in the IR with different half widths implies that the collimators are useful in shielding the lost particles due to radiative Bhabha scattering and beamstrahlung. Based on this scan, we decided to set the half width of the collimators to 8 mm and 5 mm in the horizontal and the vertical planes, respectively. However, further simulations of the accelerator and detectors need to be performed to fully estimate the effect of the collimators.

In addition, the threshold of the bunch current limited by these four collimators is about 2.1 mA according to Eq. (3). This is safe for CEPC which needs the threshold of the bunch current to be larger than 332 μA.

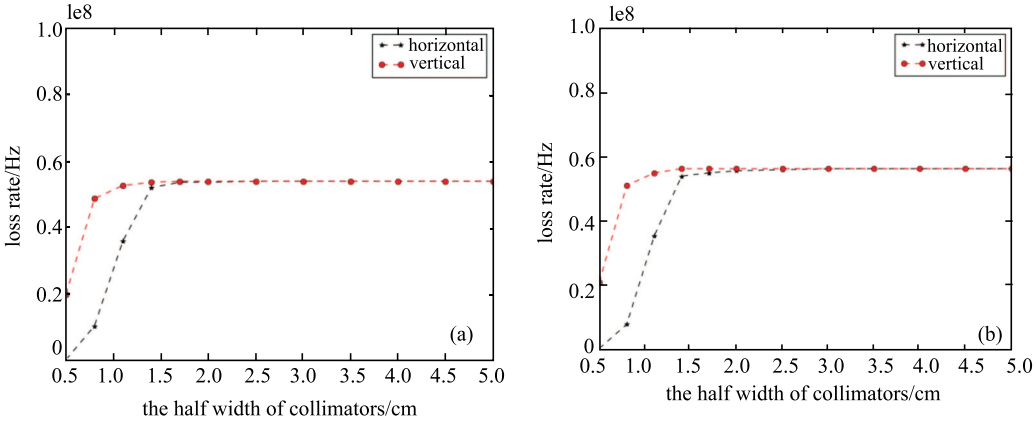

Fig. 7. (color online) Loss rate due to beamstrahlung in the IR with different half widths of collimators at the two IPs: (a) beamstrahlung originates from IP1 and (b) from IP3.

5 Simulation of background with and without collimators

5.1 Accelerator simulation

Figure 9 demonstrates the simulation results in the accelerator for radiative Bhabha scattering, showing the histogram of the position at which particles are lost in the IR in the tracking. In total, 240 turns are tracked because the transverse damping time is about 80 turns and three times damping time is long enough to detect the particles may get lost. The x-axis represents the longitudinal position with respect to the IP. The negative distances represent the region upstream of the IR. A total of 100 bins is used, each with a width of 10 cm. The y-axis gives the loss number per second per bin. A possible layout of the CEPC interaction region is shown in Fig. 8. In Fig.9, (a) and (b) represent the loss rate with and without collimators; (c) and (d) also show the loss rate with and without collimators, but with the scattering originating from IP3. From (a) to (d), one can conclude that the collimators are useful in reducing

the background in IR. The very high loss rate in downstream of the IP in (b) is because most of the events are lost in the IR immediately after the collision because of their large and sharp energy loss. The collimators are not helpful to reduce these particles. But the radiation damage and the detector background are not as serious as the loss rate for the relatively small flying angle to the ideal orbit.

Figure 10 shows the histogram of the positions at which particles are lost due to beamstrahlung in the IR in the tracking. The conclusion is similar to that from Fig. 9. In addition, we conclude that the collimators are more useful for background originating from beamstrahlung.

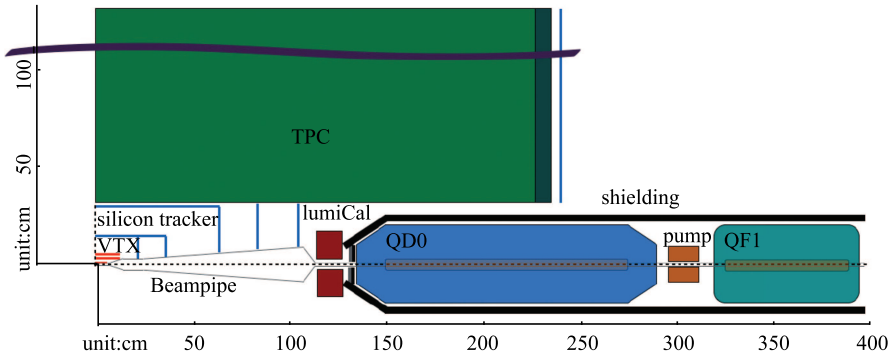

Fig. 8. Layout of the CEPC interaction region.

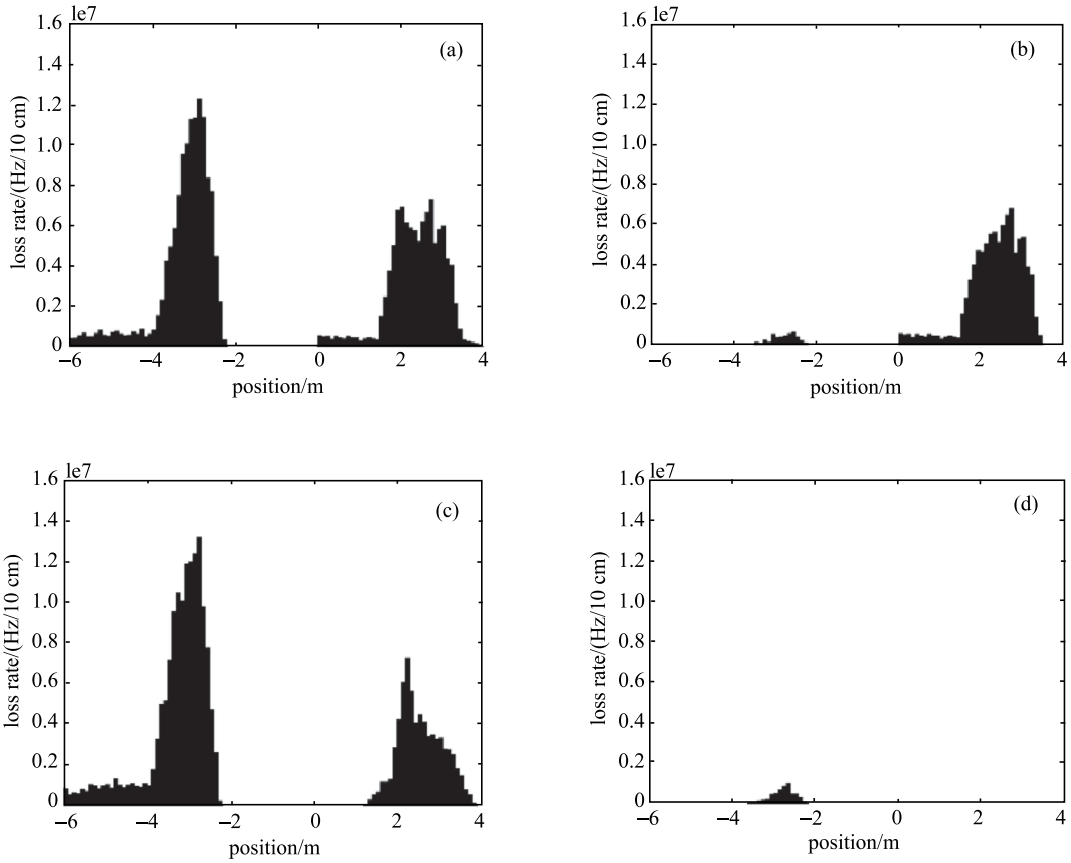

Fig. 9. Distribution of the longitudinal position at which the particles are lost in the IR. The lost particles are driven by radiative Bhabha scattering. (a) The scattering originates from IP1, simulation without collimators. (b) The scattering originates from IP1, simulation with collimators. (c) The scattering originates from IP3, simulation without collimators. (d) The scattering originates from IP3, simulation with collimators.

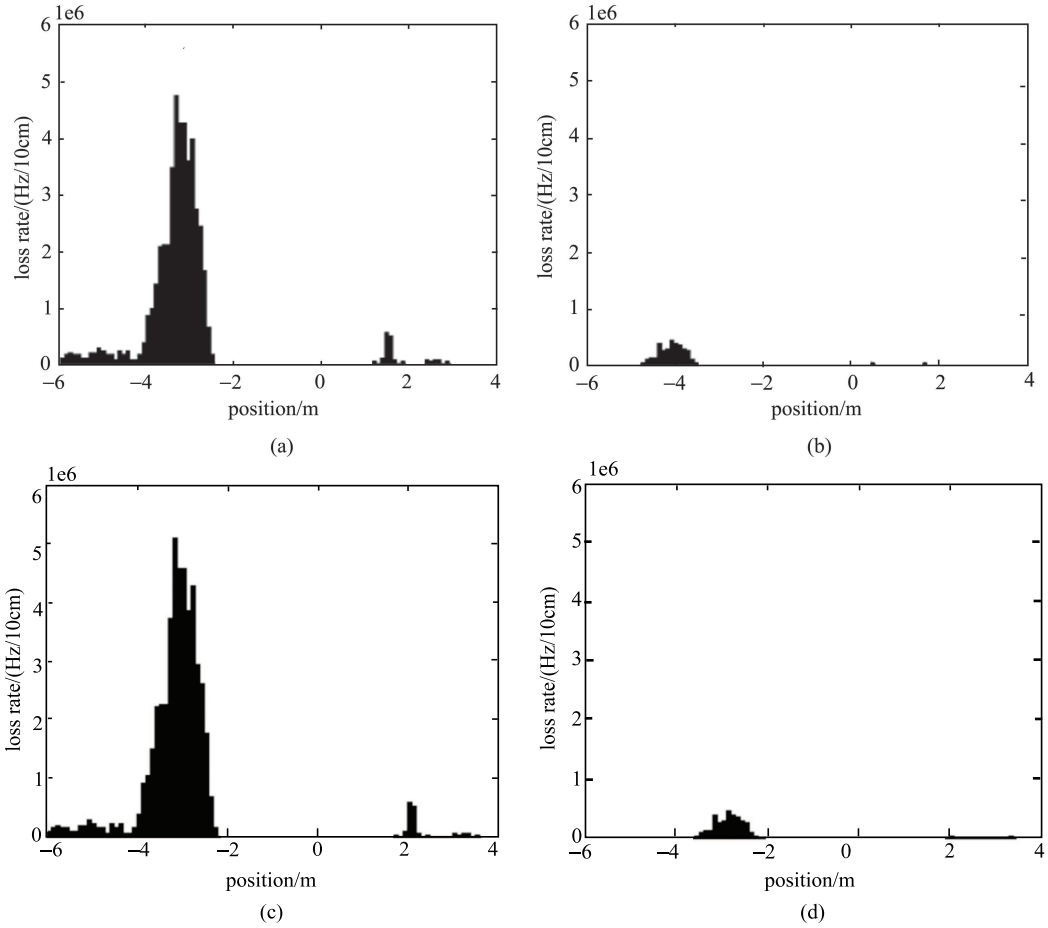

Fig. 10. Distribution of the longitudinal position where particles are lost due to beamstrahlung in the IR. (a) The beamstrahlung originates from IP1, simulation without collimators. (b) The beamstrahlung originates from IP1, simulation with collimators. (c) The beamstrahlung originates from IP3, simulation without collimators. (d) The beamstrahlung originates from IP3, simulation with collimators.

5.2 Detector simulation

In order to evaluate the influence on the detector, a detector simulation is performed using GEANT4 [14]. Because the vertex detector (VTX) is the innermost subdetector, and suffers seriously from the beaminduced background, we select the VTX as the indicator to evaluate the effects of the collimators.

Figure 11 illustrates the hit density due to radiative Bhabha scattering at the VTX with and without the collimators The black dots and green upward-pointing triangles show the results at IP1 and IP3 respectively without the collimators, while the red squares and blue downward-pointing triangles show those with the collimators mentioned above. The half widths of the collimators are 8 mm in the horizontal plane and 5 mm in the vertical plane. According to Fig. 11, the hit density at the VTX becomes around one order of magnitude lower with the collimators than without. The final hit density is confined within a tolerable level (this value should be controlled under 1 $\mathrm{cm}^{-2}\cdot\mathrm{BX}^{-1}$ if possible; slight fluctuation is acceptable). Figure 11 suggests that the preliminary design of the collimators is useful in reducing the background and radiation damage on the detectors at the CEPC.

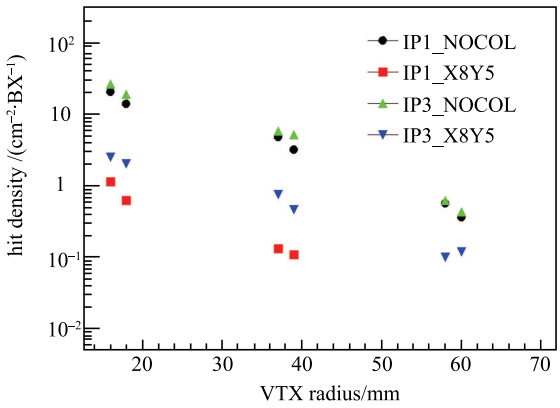

Fig. 11. (color online) Hit density due to radiative Bhabha scattering at the VTX with and without the collimators.

The simulation results at the detectors for beamstrahlung are shown in Fig. 12. A similar conclusion as for Fig. 10 can be drawn from Fig. 11, that the preliminary design of the collimators is useful in reducing the background and radiation damage on the detectors at the CEPC.

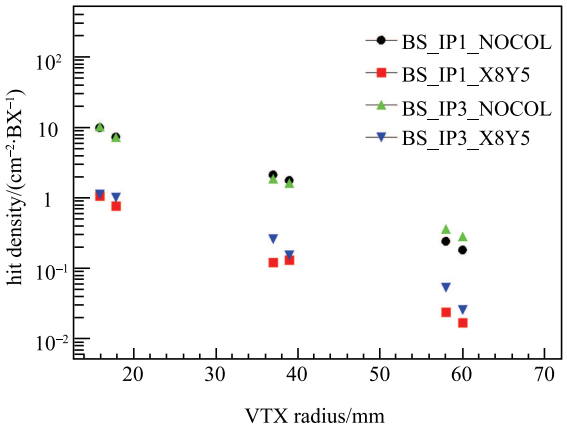

Fig. 12. (color online) Hit density due to beamstrahlung at the VTX with and without the collimators.

6 Conclusion

As a summary, the background driven by radiative Bhabha scattering and beamstrahlung are the dominant background sources at the CEPC. The collimator system is needed to protect the detectors. Considering the constraining effects, such as the constraint on the aperture, the transverse mode coupling instability condition and, for the vertical plane, the injection constraint, we can get the allowed half width and beta function space for designing the collimators. Based on the lattice at this stage, we decide to mount the horizontal collimators at DRHS12FFS.4 and DRHS22FFS.4, vertical collimators at DRHFFS.7 and DRHFFS.8. Simulating the loss rate in the IR with different half widths of the collimators, we preliminarily set the half width of the collimators to 8 mm and 5 mm in the horizontal and vertical planes respectively. The further simulation of the accelerator and detectors demonstrates that the collimators we designed are useful in shielding the two main backgrounds mentioned above.

The authors would like to thank Wang Na, Sun Yuansheng and Bai Sha for helpful discussions Funakoshi-san for the help on the usage of SAD, and Zhou Demin for the help on the impedance of collimators.

References

1 ATLAS Collaboration, Phys. Lett. B, **716**: 1–29, 2012
2 CMS Collaboration, Phys. Lett. B, **716**: 30–61, 2012
3 https://fcc.web.cern.ch/Pages
4 The CEPC-SPPC Study Group, *CEPC-SPPC Preliminary Conceptual Design Report*, Volume II-Accelerator
5 T. Yue, Q. Qin, Study of Background and MDI Design for CEPC.in *Proceedings of the Seventh International Particle Accelerator Conference*, (Richmond, America, 2015)
6 A. W. Chao, M. Tigner, *Handbook of Accelerator physics and engineering*, (3rd Printing), p 136
7 A. M. Toader, R. Barlow Comparison of Collimator Wakefields Formulae, in *Proceedings of 11th European Particle Accelerator Conference* (Genoa, Italy, 2008)
8 G. V. Stupakov High-Frequency Impedance of Small-Angle Collimators in *Proceedings of the 2001 Particles Accelerator Conference* (Chicage, America)
9 Y. W. Wang, X. H. Cui, J. Gao, IHEP preprint, IHEP-AC-LC-Note2015-015
10 R. Kleiss, H. Burkhardt, CERN preprint, CERN-SL-94-03(OP)
11 SAD. http://acc-physics.kek.jp/SAD/
12 V. I. Telnov Phys. Rev. Letters, **110**: 114801(2013)
13 A. Bogomyagkov, E. Levichev, and D. Shatilov Phys. Rev. ST Accel. Beams, **17**: 041004 (2014)
14 GEANT4 Collaboration, Nucl. Instrum. Methods A, **506** (2003)